



CH₄ and CO distributions over tropical fires during October 2006 as observed by the Aura TES satellite instrument and modeled by GEOS-Chem

J. Worden¹, K. Wecht², C. Frankenberg¹, M. Alvarado³, K. Bowman¹, E. Kort¹, S. Kulawik¹, M. Lee¹, V. Payne¹, and H. Worden⁴

¹Jet Propulsion Laboratory/California Institute of Technology, Pasadena, California, USA

²Harvard University, Cambridge, Massachusetts, USA

³Atmospheric and Environmental Research, Lexington, Massachusetts, USA

⁴National Center for Atmospheric Research, Boulder, Colorado, USA

Correspondence to: J. Worden (john.worden@jpl.nasa.gov)

Received: 8 September 2012 – Published in Atmos. Chem. Phys. Discuss.: 5 October 2012

Revised: 23 January 2013 – Accepted: 5 March 2013 – Published: 3 April 2013

Abstract. Tropical fires represent a highly uncertain source of atmospheric methane (CH₄) because of the variability of fire emissions and the dependency of the fire CH₄ emission factors (g kg⁻¹ dry matter burned) on fuel type and combustion phase. In this paper we use new observations of CH₄ and CO in the free troposphere from the Aura Tropospheric Emission Sounder (TES) satellite instrument to place constraints on the role of tropical fire emissions versus microbial production (e.g. in wetlands and livestock) during the (October) 2006 El Niño, a time of significant fire emissions from Indonesia. We first compare the global CH₄ distributions from TES using the GEOS-Chem model. We find a mean bias between the observations and model of 26.3 ppb CH₄ that is independent of latitude between 50° S and 80° N, consistent with previous validation studies of TES CH₄ retrievals using aircraft measurements. The slope of the distribution of CH₄ versus CO as observed by TES and modeled by GEOS-Chem is consistent (within the TES observation error) for air parcels over the Indonesian peat fires, South America, and Africa. The CH₄ and CO distributions are correlated between $R = 0.42$ and $R = 0.46$, with these correlations primarily limited by the TES random error. Over Indonesia, the observed slope of $0.13 \text{ (ppb ppb}^{-1}) \pm 0.01$, as compared to a modeled slope of $0.153 \text{ (ppb ppb}^{-1}) \pm 0.005$ and an emission ratio used within the GEOS-Chem model of approximately $0.11 \text{ (ppb ppb}^{-1})$, indicates that most of the observed methane enhancement originated from the fire. Slopes of

$0.47 \text{ (ppb ppb}^{-1}) \pm 0.04$ and $0.44 \text{ (ppb ppb}^{-1}) \pm 0.03$ over South America and Africa show that the methane in the observed air parcels primarily came from microbial-generated emissions. Sensitivity studies using GEOS-Chem show that part of the observed correlation for the Indonesian observations and most of the observed correlations over South America and Africa are a result of transport and mixing of the fire and nearby microbial-generated emissions into the observed air parcels. Differences between observed and modeled CH₄ distributions over South America and southern Africa indicate that the magnitude of the methane emissions for this time period are inconsistent with observations even if the relative distribution of fire versus biotic emissions are consistent. This study shows the potential for estimation of CH₄ emissions over tropical regions using joint satellite observations of CH₄ and CO.

1 Introduction

Atmospheric methane (CH₄) concentrations have increased nearly three-fold since pre-industrial times, largely attributable to gas exploration, coal mining, rice agriculture, waste handling, and an increased population of ruminants (Forster et al., 2007). Methane concentrations stabilized in 1999 (Rigby et al., 2008) but then began increasing again in 2007 for essentially unknown reasons. For example, the

persistence of the increase between 2007 and 2012 casts doubt on earlier hypotheses of anomalous rainfall and temperature patterns as the culprit (Rigby et al., 2008; Dlugokencky et al., 2009; Bloom et al., 2010; Bousquet et al., 2011).

It is now recognized that one of the most efficient methods to mitigate warming due to greenhouse gases on decadal time frames is to cut methane emissions (e.g., Shindell et al., 2012) as the warming potential for methane is 72 times higher than carbon dioxide (CO₂) on a 20 yr time horizon (e.g., Forster et al., 2007; Lelieveld et al., 1998). The dominant CH₄ sink is oxidation by OH radicals in the atmosphere, resulting in a short 9 yr lifetime (e.g., Fung et al., 1991); reducing methane emissions thus rapidly lowers its atmospheric abundance. Quantifying anthropogenic and natural methane emissions is thus critical for identifying methane emission reduction targets, verifying that these target have been met, and understanding climate/carbon cycle feedbacks, as increased warming can lead to increased high-latitude methane emissions from the soil or from biomass burning (e.g., O'Connor et al., 2010, and references therein).

Approximately half of the annual 550 Tg yr⁻¹ methane emissions are anthropogenic, with the bulk of these anthropogenic emissions distributed in the northern mid-latitudes (e.g., Fung et al., 1991; Lelieveld et al., 1998; Bousquet et al., 2006). Bottom-up quantification of emissions is intrinsically more difficult for methane than for CO₂ because most non-energy-related CH₄ emissions are biogenic, i.e. the CH₄ is created by microbes (methanogens) in anaerobic habitats such as wetlands, landfills, agricultural soils, rice paddies, and the stomachs of ruminants. Consequently, uncertainties in natural and anthropogenic emissions can exceed 100% (e.g., Petron et al., 2012).

Fires, though not a dominant source of methane (e.g., Forster et al., 2007; Dlugokencky et al., 2011), represent a significant contributor to the seasonal variability of atmospheric methane (e.g., Bousquet et al., 2006). The year 2006 was a time of significant tropical peat fire emissions over Indonesia due to a strong El Niño (e.g., Page et al., 2002; Logan et al., 2008; Nassar et al., 2009; Gonzi and Palmer, 2010). For example, carbon monoxide emissions from these Indonesian fires for October 2006 were approximately six times larger than in October 2005 (Logan et al., 2008). Figure 1 shows the October 2006 monthly average of surface and middle-tropospheric atmospheric CO concentrations from the Terra Measurement of Pollution in the Troposphere (MOPITT) satellite instrument (Worden et al., 2010; Deeter et al., 2011, 2012). Enhanced values of CO are observed at the surface in Indonesia and are significantly enhanced in the free troposphere relative to biomass burning regions over South America and Africa. The plumes from these enhanced fire emissions were also observed in the upper troposphere by the Microwave Limb Sounder (MLS) (e.g. Gonzi and Palmer, 2010). These combined observations from the surface, free troposphere, and upper troposphere therefore show that the

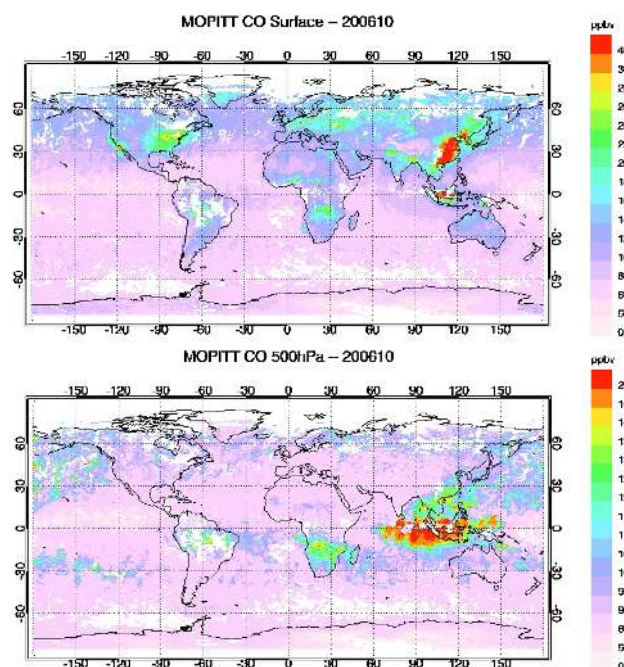


Fig. 1. (a) Surface CO estimates (version 5 release) from the Terra MOPITT satellite for October 2006. (b) Tropospheric CO estimates (version 5 release) from the Terra MOPITT satellite for October 2006.

strong Indonesian biomass burning emissions, coupled with convection, resulted in nearly the whole tropospheric column over the fire being affected by the smoke plume (Logan et al., 2008; Nassar et al., 2009).

Despite recent advances in quantifying the global distribution of methane emissions from space (e.g., Frankenberg et al., 2005, 2011; Xiong et al., 2009; Crevoisier et al., 2009), challenges remain in quantifying methane emissions from fires because of the difficulty in identifying methane enhancements in smoke plumes. The surface network is also challenged to place constraints on tropical fire emissions because fire plumes are lofted into the free troposphere (e.g., Dlugokencky et al., 2009). In this paper we use new measurements of tropospheric methane from the Aura TES satellite instrument, as well as TES observations of CO, to quantify the enhancement of CH₄ relative to CO over regions of tropical biomass burning during October 2006.

The TES CH₄ estimates (derived from thermal infrared radiance measurements as described in Sect. 2 and Worden et al., 2012) are primarily sensitive to CH₄ concentrations and variability in the free troposphere and have little sensitivity to near-surface CH₄ variations. However, tropical fire plumes are rapidly advected or convected into the free troposphere where the TES CH₄ estimates have maximum sensitivity. In addition, the TES estimates are mostly insensitive to biomass burning aerosols because the corresponding aerosol optical depth (AOD) is negligible at thermal wavelengths

(AOD < 0.01) as the AOD likely depends on $1/\lambda^2$ (Kirchstetter et al., 2004). Furthermore, under the conservative assumption that the AOD might be larger than 0.01 at thermal wavelengths, the effect of AOD on the retrieval would be characterized with the cloud-component of the TES retrieval (Kulawik et al., 2006; Eldering et al., 2008; Verma et al., 2009; Worden et al., 2012).

Our motivation with this analysis is to test both the skill of the retrievals in quantifying methane variations in tropical smoke plumes and to test the skill of the GEOS-Chem global atmospheric chemistry model to quantify methane emissions and the subsequent dispersion of the plume. For these tests, we use TES estimates of CH₄ and CO (e.g., Worden et al., 2004, 2012; Logan et al., 2008; Ho et al., 2009; Luo et al., 2010) to investigate correlations and to quantify the ratio of the enhancements of CH₄ and CO over tropical fires in South America, southern Africa, and Indonesia. The approach discussed in this paper will be used in subsequent analysis for quantifying the relative role of fires, wetlands, and transport on the observed methane distributions, and when possible, to quantify the methane emissions from the fires.

2 Description of TES instrument and CH₄ estimates

The TES instrument is an infrared, high spectral resolution, Fourier Transform spectrometer covering the spectral range between 650 and 3050 cm⁻¹ (15.4 to 3.3 μm) with an apodized spectral resolution of 0.1 cm⁻¹ for the nadir view (Beer et al., 2001). Spectral radiances measured by TES are used to infer atmospheric profiles using a non-linear optimal estimation algorithm that minimizes the difference between these radiances and those calculated with the equation of radiative transfer (Clough et al., 2006), subject to the constraint that the parameters are consistent with a statistical a priori description of the atmosphere (Bowman et al., 2006). TES provides a global view of tropospheric trace gas profiles including ozone, water vapor and its isotopes, carbon monoxide and methane, along with atmospheric temperature, surface temperature, surface emissivity, effective cloud top pressure, and effective cloud optical depth (Worden et al., 2004, 2012; Kulawik et al., 2006; Eldering et al., 2008).

2.1 Vertical resolution and error characteristics of TES CH₄ and CO

2.1.1 CH₄ vertical resolution and calculated errors

Details of the TES CH₄ retrieval are discussed in Worden et al. (2012). In this paper we use TES CH₄ “version 5” profiles. In particular we use the “Lite” products available at <http://tes.jpl.nasa.gov/data> in which the TES Level 2 (single observation) data are (1) collected into monthly files, (2) at reduced dimensionality relative to the original TES data products, and (3) bias corrected using co-retrieved N₂O estimates. For this CH₄ retrieval, the logarithm of the vol-

ume mixing ratio (VMR) of CH₄ is simultaneously estimated along with cloud optical depth, cloud-top pressure, surface temperature and the logarithm of the VMR of H₂O, HDO, and N₂O. By jointly estimating CH₄ with N₂O, systematic uncertainties related to temperature, calibration, and H₂O can be mitigated in the CH₄ estimate by referencing the CH₄ estimate to the N₂O estimate because the vertical distribution of the sensitivities of thermal IR radiances in the 8 μm band to CH₄ and N₂O are similar (Worden et al., 2012).

TES CH₄ estimates are primarily sensitive to free-tropospheric CH₄ (between approximately 850 hPa and the tropopause) with some sensitivity to the boundary layer and stratosphere as shown by a typical averaging kernel for a tropospheric CH₄ estimate in Fig. 2. The averaging kernel (left panel of Fig. 2) describes the sensitivity of the (log) CH₄ estimate to the “true” distribution of (log) CH₄. As discussed in Rodgers (2000), a metric for the sensitivity of a remotely sensed estimate is the degrees-of-freedom for signal (DOFS) that describes the number of pieces of information in a retrieval. For the TES trace gas estimates, the estimated parameters are usually the log of the trace gas concentration in volume mixing ratio, or log(VMR), which is primarily sensitive to variations in the trace gas. Therefore, a DOFS of 1 for indicate that the retrieval can resolve variations of methane within the calculated random errors. Generally, larger values of the DOFS indicate increased vertical resolution of the estimate.

As discussed in Worden et al. (2012), we assume for the methane constraint used in the TES methane retrievals that the free-troposphere CH₄ can vary by as much as 5% from our a priori knowledge but that CH₄ is also relatively well mixed in the troposphere. These assumptions affect both the corresponding averaging kernel (or vertical sensitivity) and the vertical distribution of uncertainties for the CH₄ estimate as shown in Fig. 2 (right panel, taken from Worden et al., 2012). The dominant uncertainty in the lower troposphere is due to errors in the TES temperature estimate. In the upper troposphere, the dominant random uncertainty is due to noise in the measured radiances.

2.1.2 Validation of TES CH₄ bias and random error with HIPPO data

TES CH₄ estimates have been validated using aircraft CH₄ profiles from the HIAPER Pole-to-Pole Observation (HIPPO) mission (Wecht et al., 2012). According to Wecht et al. (2012), the TES data in the upper troposphere and lower troposphere have different biases which potentially vary by latitude, with the lower-tropospheric methane in the tropics (20° S to 20° N) biased high by approximately 16.9 ppb and the higher latitudes biased high by 28.8 ppb.

Worden et al. (2012) also show that the vertical distribution of TES CH₄ is biased high in the upper troposphere relative to the lower troposphere by 2.8%. This bias is possibly due to temperature errors in the methane spectroscopy

(Worden et al., 2004, 2012). In order to reduce the effects of this vertically distributed bias error, we average the retrieved VMRs of CH₄ and CO throughout the troposphere (i.e., from the surface to the tropopause) before comparing the TES retrievals to GEOS-Chem, as discussed in Sects. 4 and 5. We do not compute a total column average from these profiles because a column average would be strongly weighted towards the boundary layer where the TES data typically have little sensitivity. In the analysis discussed in this paper we examine the bias with respect to GEOS-Chem (Sect. 4) by comparing averages of the model and data and find that the biases vary little with respect to latitude and therefore have negligible effect on the comparisons made in this paper.

Wecht et al. (2012) also find that the actual random uncertainty, as calculated through the root-mean-square difference between HIPPO and TES data, is larger than the calculated uncertainty as described in Fig. 2. However, this difference could result from the dependency of the TES tropospheric CH₄ estimates on stratospheric CH₄ variations and the HIPPO mission did not typically measure CH₄ in the stratosphere. Consequently, uncertainties in the assumed stratospheric CH₄ distribution used for comparing HIPPO data to TES data can result in larger differences between the TES and HIPPO CH₄ comparisons than expected (this is called extrapolation error in the Wecht et al. (2012) study). As can be inferred from the right panel of Fig. 2, the calculated random uncertainty in these averaged profiles from the surface to the tropopause ranges from approximately 0.5 % to 2 % with the error depending on measurement noise, the distribution of radiative interferences, and temperature. We use these calculated uncertainties for the analysis discussed in this paper. The errors for a tropospheric average of CH₄ and CO is calculated by averaging the calculated observation error covariance: $\delta_{\text{ch}_4} = [(N^{-1}S_{\text{obs}}(N^{-1})^T]^{1/2}$, where δ_{ch_4} is the fractional error of the tropospheric average, N is a vector that is the same length as the number of pressure levels between the surface to the tropopause, and each element of this vector is $1/N$, with N being the number of pressure levels. The S_{obs} is the observation error covariance, contained in all the TES product files, (Worden et al., 2004, 2012) that characterizes the estimated uncertainties and their cross-correlations due to noise, temperature, and the primary radiative interferences such as clouds and H₂O. Note that the smoothing error due to the limited vertical resolution of the TES estimates is not considered in this tropospheric average because comparisons between data and model can explicitly account for the smoothing error by application of the instrument operator to the model (see Sect. 4.1).

2.1.3 CO

Details of the vertical resolution, error characteristics, and validation of the TES CO estimates can be found in Luo et al. (2007). Similar to the TES CH₄ estimates, the TES CO estimates have peak sensitivity to the middle troposphere with

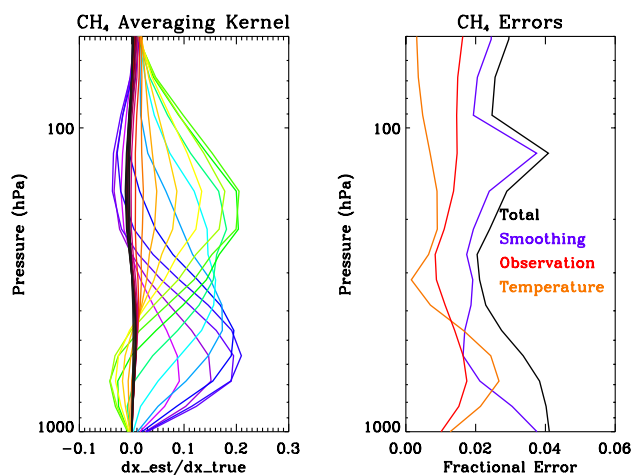


Fig. 2. (Left panel) Averaging kernels for TES estimate of CH₄ for tropical scene. Different colors help to distinguish pressures corresponding to each averaging kernel. (Right panel) Error distribution for TES CH₄ estimate for tropical scene. The observation error includes uncertainties from noise and interferences such as H₂O.

little sensitivity to the boundary layer or to the stratosphere. The DOFS of the TES CO estimates range from approximately 0.8 to 1.5 for latitudes ranging from ± 50 degrees to the equator. A tropospheric average of the TES CO profile, in VMR, typically has an uncertainty of 2.5 %. As discussed in Luo et al. (2007) biases in the TES CO data are not evident and so are not considered in this analysis.

3 Description of GEOS-Chem

GEOS-Chem is a global 3-D chemical transport model driven by GEOS-assimilated meteorological data from the NASA Global Modeling and Assimilation Office (GMAO) (<http://acmg.seas.harvard.edu/geos/>). The model was originally described by Bey et al. (2001). In this study, we run GEOS-Chem version 9-01-02 with GEOS-5 meteorological data at $2^\circ \times 2.5^\circ$ (lat, lon) horizontal resolution with 47 vertical layers and a time resolution of 6 h. The GEOS-Chem methane simulation was developed by Wang et al. (2004) and updated by Pickett-Heaps et al. (2011). Model methane concentrations are initialized using observations from the NOAA/GMD surface network and were simulated for twenty years prior to use in this study. Model methane sources include anthropogenic emissions from EDGAR 4.0 (European Commission, 2009), GFED2 biomass burning emissions (van der Werf et al., 2006), and natural wetland emissions based on Kaplan (2002) and described by Pickett-Heaps et al. (2011). We compute the loss of methane from reaction with the OH radical using monthly mean 3-D OH concentration fields as discussed in Park et al. (2004). The global mean tropospheric OH concentration is 10.8×10^5 molec cm⁻³, as constrained by methyl chloroform measurements (Prinn et

al., 2005). Additional minor sinks include prescribed stratospheric loss rates (Wang et al., 2004) and soil absorption (Fung et al., 1991). The GEOS-Chem methane lifetime is 9.5 yr, consistent with the lifetime of 8.7 ± 1.3 yr reported by Denman et al. (2007).

4 Comparison of TES to GEOS-Chem global distributions

4.1 Comparison approach

The first primary step to comparing the TES data to GEOS-Chem model profiles is to find the nearest spatio-temporal match between observation and model. As discussed in Sect. 3, the GEOS-Chem model grid spacing is 2×2.5 degrees with a temporal resolution of 6 h. The next primary step is to account for the a priori constraint and vertical resolution of the TES estimate, or else differences between the remotely sensed estimate and the model will be driven by choices in the a priori constraint instead of process errors in the model or errors in the retrieval from noise or interferences (e.g., Rodgers and Connor, 2003). We account for the effects of the a priori constraint and vertical resolution by applying the TES instrument operator to the GEOS-Chem model profile:

$$\hat{x}_{GC} = x_a + \mathbf{A}(x_{GC} - x_a), \quad (1)$$

where \mathbf{A} is the TES averaging kernel matrix (e.g., left panel of Fig. 2) for the CH₄ estimate, x_a is the logarithm of the a priori profile used for the TES retrieval and x_{GC} is the logarithm of the GEOS-Chem CH₄ profile. After applying the TES instrument operator, the difference between the TES estimate and the GEOS-Chem profile will be the uncertainties in the TES estimate which are due to noise, temperature, and radiative interferences such as H₂O and clouds (Eq. 3 in Worden et al., 2012) along with uncertainties in the model estimate.

We also find that errors in the GEOS-Chem stratospheric distribution of methane can strongly affect the comparison between the TES and GEOS-Chem tropospheric methane distributions, even after accounting for the TES a priori constraint and averaging kernel. For example, Fig. 3 shows a comparison between a sample TES and GEOS-Chem profile over a region in South America with significant methane enhancement in the boundary layer. After the full (surface to top-of-atmosphere) TES instrument operator (Eq. 1) has been applied to the GEOS-Chem profile (black line), the GEOS-Chem estimate peaks in the upper troposphere, whereas the TES profile peaks in the middle/lower troposphere. We find that the orders-of-magnitude differences between the GEOS-Chem methane distribution in the upper stratosphere (pressures less than 50 hPa) and the TES a priori have a significant impact on comparison in the troposphere even though the averaging kernel values at these stratospheric pressure levels are quite small.

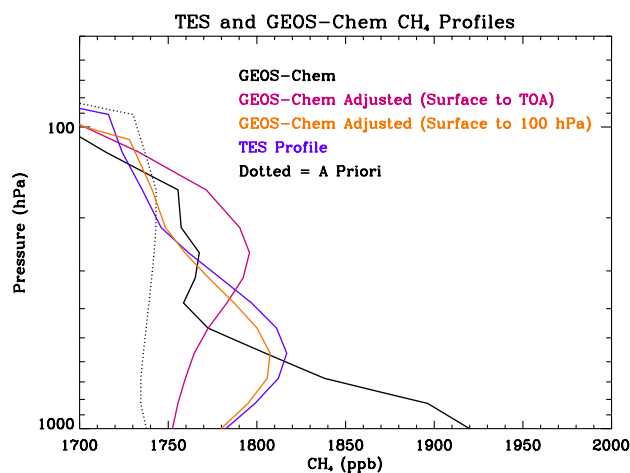


Fig. 3. Comparison of TES and GEOS-Chem profiles. (Black) GEOS-Chem CH₄ profile over S. America over region of enhanced biomass burning. The red line shows the GEOS-Chem profile after applying the TES constraint vector and full averaging kernel (from surface to the top of atmosphere). The orange line shows the GEOS-Chem profile if only the averaging kernels from the surface to 100 hPa are applied to the GEOS-Chem profile. The TES profile is shown in blue and the a priori is the dotted line.

In order to mitigate this numerical error due to large differences between the a priori and the GEOS-Chem upper stratospheric methane distributions, the averaging kernels and model fields are first truncated near the tropopause (or 80 hPa) before applying the TES averaging kernel and a priori (the TES operator) to the GEOS-Chem fields. Not accounting for the stratosphere is equivalent to replacing the GEOS-Chem stratosphere with the TES a priori stratosphere as seen in Eq. (1). Because we no longer apply the stratospheric component of the averaging kernel and a priori constraint to the model fields, we have replaced one uncertainty due to GEOS-Chem stratospheric model error with another uncertainty that is due to stratospheric variations on the TES methane estimate. This error is called “cross-state” error in Worden et al. (2004) because it is the error from jointly estimating one set of parameters (i.e., stratospheric methane) with another set of parameters (i.e., tropospheric methane). We can estimate the effect of this error on our comparison between TES and GEOS-Chem by using the assumed covariance for the TES methane a priori in the stratosphere and the TES averaging kernels and find that the magnitude of the error is on the order of 3 ppb or less; consequently we ignore the error as it is negligible relative to the errors from noise, H₂O, clouds, and temperature. After applying the truncated averaging kernel to the GEOS-Chem profile, the vertical distribution of the GEOS-Chem estimate in the troposphere peaks lower in the troposphere (orange curve in Fig. 3) and is more comparable to the TES observations for this particular observation. Future versions of the GEOS-

Chem model will have an improved estimate of stratospheric methane and we expect that we will not need to apply this correction when using these improved model fields. Note that the effect of the averaging kernel matrix and a priori on the GEOS-Chem profile increases the middle-tropospheric CH₄ values while greatly reducing the boundary layer values because the a priori does not have the same boundary layer distribution and the averaging kernel shows little sensitivity to the boundary layer.

Two final retrieval and model characteristics that are empirically found to affect the TES and GEOS-Chem methane/CO comparisons are that the vertical sensitivity of the TES CH₄ and CO estimates vary differently by altitude and that uncertainties in the GEOS-Chem vertical transport can place CO or methane at incorrect altitudes. We mitigate these effects of these data and model differences on the comparison by averaging the TES and GEOS-Chem CH₄ profiles from the surface to the tropopause after applying the instrument operator to the GEOS-Chem profile. We can quantify the effect of these averaging operations on our conclusions by comparing the GEOS-Chem CO/CH₄ distributions before applying the TES operator to the GEOS-Chem distributions after applying the TES instrument operator as discussed in Sect. 5.

4.2 Latitudinal variability of biases in TES and GEOS-Chem CH₄ comparisons

In this section we compare the latitudinal distribution of TES and GEOS-Chem CH₄ estimates in order to globally evaluate how potential errors in the TES stratospheric CH₄ estimate or the tropopause height could affect GEOS-Chem and TES comparisons. Note that this error affects the TES estimate only and is different from that discussed in the previous section in which it was found that large differences between the GEOS-Chem CH₄ and TES a priori in the stratosphere could affect the comparisons between model and data. Figure 4 shows the TES CH₄ estimates as compared to the GEOS-Chem values (with the averaging kernel applied) as a function of latitude. Each data point is the average of the CH₄ VMR from the surface to the tropopause. All data in which the retrieval converged and the DOFS are larger than 1.2 are used to ensure that the TES estimate is sensitive to the tropospheric CH₄ variations. The mean difference is approximately 26.3 ± 0.5 ppb for all data north of 50° S. This bias is consistent with the comparison of the TES CH₄ data to the HIPPO data, which showed a similar high bias in the TES retrievals (Wecht et al., 2012). However, the mean difference becomes larger at latitudes south of 60° S, primarily due to relatively high TES CH₄ data. As discussed previously, the random error due to noise and co-retrieval of interferences is approximately between 8 and 20 ppb, thus indicating that much of the observed variance is likely due to variations in atmospheric methane.

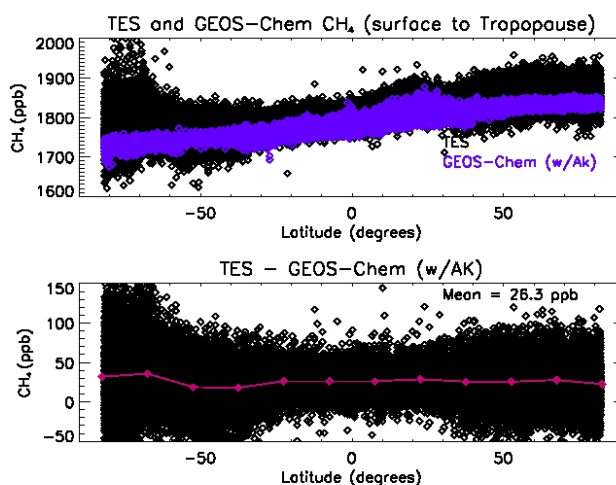


Fig. 4. (Top panel) Latitudinal distribution of TES October 2006 tropospheric CH₄ estimates (black diamonds) corresponding to GEOS-Chem estimates adjusted with TES instrument operator (blue diamonds). (Bottom panel) Difference between TES and adjusted GEOS-Chem estimates (black – blue from top panel). The red line in the bottom panel shows the mean difference between TES and the adjusted GEOS-Chem estimates when these differences are averaged for data within 15-degree latitude bins.

It is possible that poor specification of the tropopause height in the TES a priori CH₄ distribution at these higher latitudes could contribute to these differences as incorrect tropopause height would lead to strong differences between the TES CH₄ a priori in the stratosphere and the true CH₄ distribution which can then propagate to the tropospheric part of the TES methane estimate. For example, the bottom panel of Fig. 5 shows the contribution from CH₄ variations in the stratosphere to the TES tropospheric estimate at 562 hPa. These values are calculated by summing the averaging kernel corresponding to 562 hPa for pressures lower than the average tropopause pressure (red line in top panel of Fig. 5) and dividing it by the sum of the 562 hPa averaging kernel. Differences between the TES CH₄ a priori and the “true” CH₄ distribution in the stratosphere will have a larger effect on the TES CH₄ tropospheric estimate for larger values shown in the bottom panel of Fig. 5. Lower values in the Southern Hemisphere south of 60° S are likely in error because of the lower altitude (higher pressure) tropopause heights at these latitudes. For these reasons we remove all data in subsequent comparisons for latitudes south of 50° S and if the stratospheric contribution, as described in the bottom panel in Fig. 5, is larger than 0.3.

We are currently assimilating the TES data into the GEOS-Chem model for comparison with the HIPPO data, using the mapping and data quality assessment approaches discussed in this paper, in order to re-evaluate the bias in the TES data and attribute its sources; this analysis builds on the study by Wecht et al. (2012) and will be the subject of a future paper.

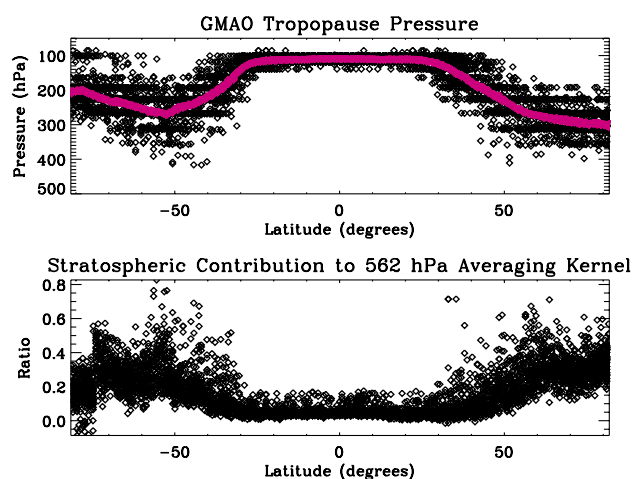


Fig. 5. (Top panel) Tropopause height from GMAO. The red line is the latitudinal average. (Bottom panel) Contribution of stratospheric differences between TES a priori and “true” CH₄ distributions to the TES tropospheric CH₄ estimate at 562 hPa.

However, we do not expect these errors to affect the study presented here as we focus on the tropics where, as seen in Fig. 5, the bias is stable and the error on the mean of the bias is less than 1 ppb. In addition, the effect of stratospheric variability on the TES tropospheric CH₄ estimates is small and the tropopause height is well measured and stable across the tropics.

4.3 Maps of TES and GEOS-Chem CH₄ and CO estimates

Prior to using the GEOS-Chem model to compare to the TES data over specific regions such as fires, it is useful as a “sanity check” to compare the data globally to ensure that both data and model show the same features, especially in the region of interest (the tropics). Figure 6 shows global maps of TES CH₄ tropospheric average estimates for October 2006 (Fig. 6a) along with the corresponding GEOS-Chem CH₄ distributions, after applying the truncated TES instrument operator described by Eq. (1) (Fig. 6b) and the difference between the two (Fig. 6c). We use the same quality flags and averaging approach discussed in Sects. 4.1 and 4.2. The individual GEOS-Chem CH₄ model values in Fig. 6b are selected by finding the closest match in time and space to the individual TES observations. Figure 7 shows global maps of CO; individual CO data used to generate this map correspond in time and space to the individual CH₄ data used to generate Fig. 6. Figure 8 shows the a priori distributions used to regularize the TES CH₄ (top panel) and CO (bottom panel) estimates. The CH₄ TES data in Fig. 6 have been bias corrected using the mean value of 26.3 ppb shown in Fig. 4 (bottom panel). All estimates are averaged within each 2° × 2.5° grid box, and only grid boxes with at least 4 TES

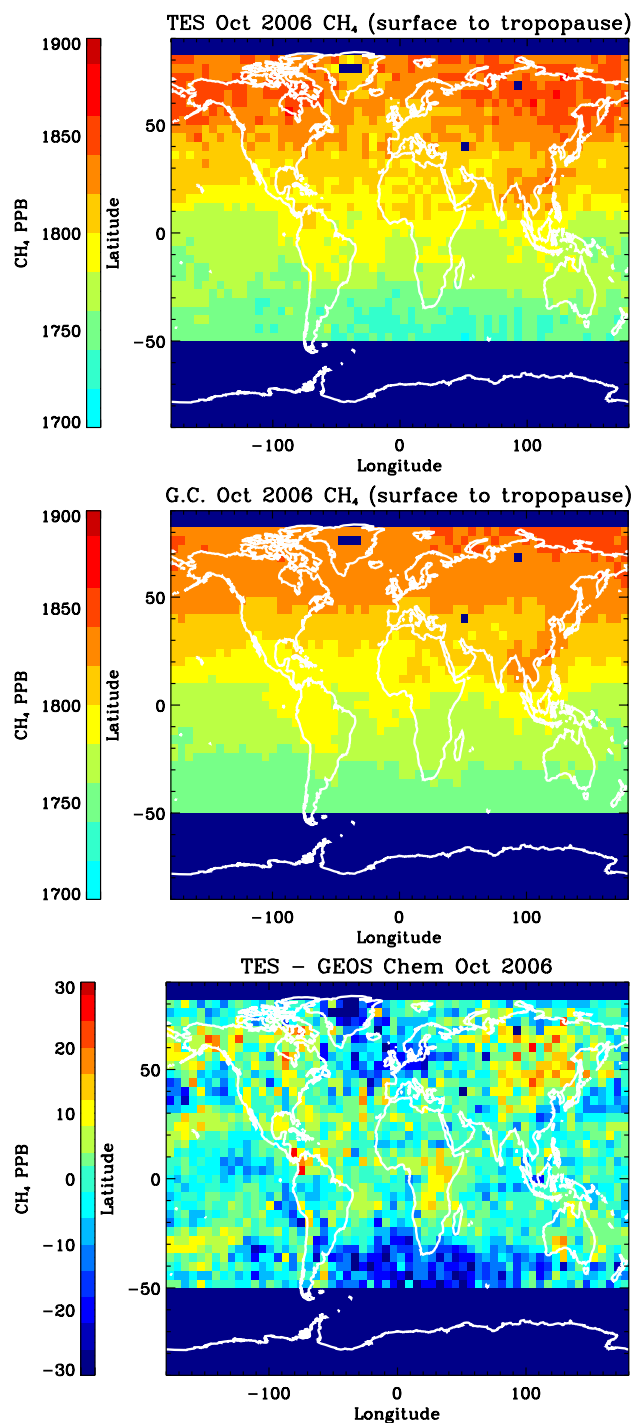


Fig. 6. (a) TES tropospheric CH₄ estimates. The TES estimates have been reduced by 26.3 ppb. (b) Corresponding GEOS-Chem CH₄ estimates adjusted with the TES instrument operator. (c) Difference between TES and GEOS-Chem.

observations are shown in the map. The GEOS-Chem CO values have been decreased by 19.9 ppb to account for the mean global bias between TES and GEOS-Chem CO estimates and to be consistent with previous studies indicating

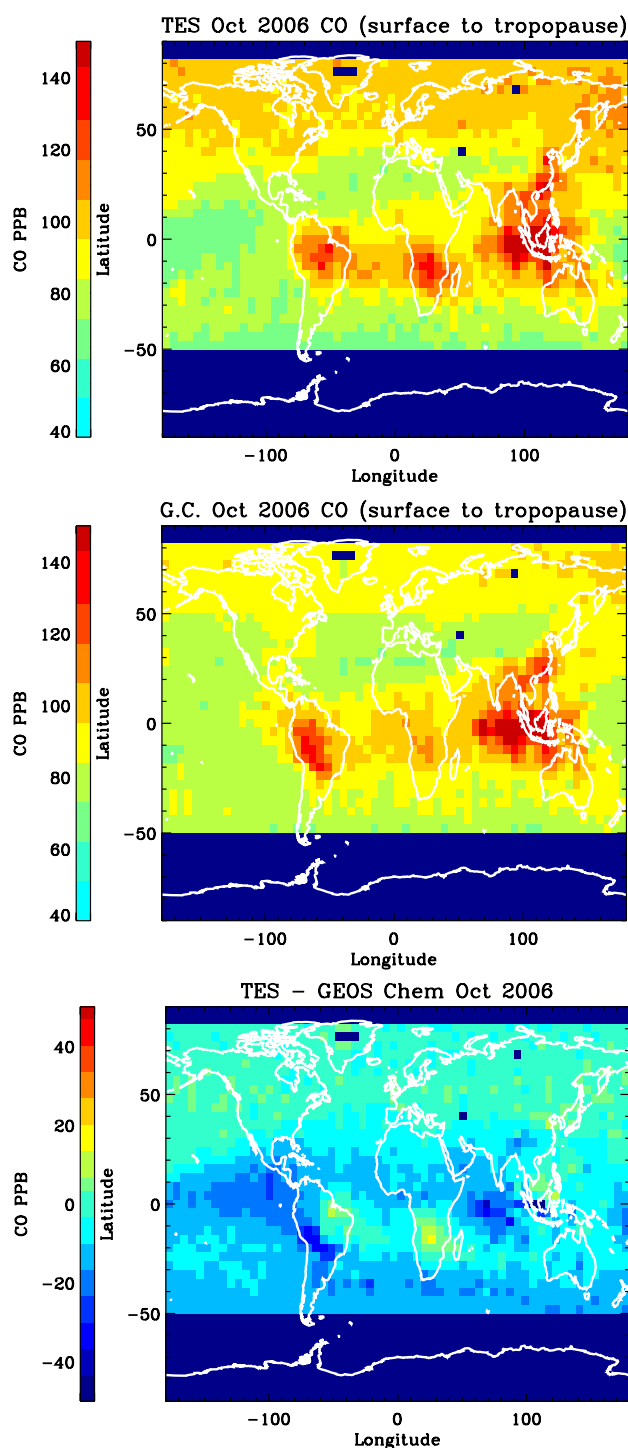


Fig. 7. (a) TES tropospheric CO estimates. (b) Corresponding GEOS-Chem CO estimates adjusted with the TES instrument operator. The GEOS-Chem values have been reduced by 19.9 ppb. (c) Difference between TES and GEOS-chem.

that TES data are effectively unbiased with respect to independent data sets (Luo et al., 2007). Unlike with the methane estimates, this bias in CO shows regional and latitudinal vari-

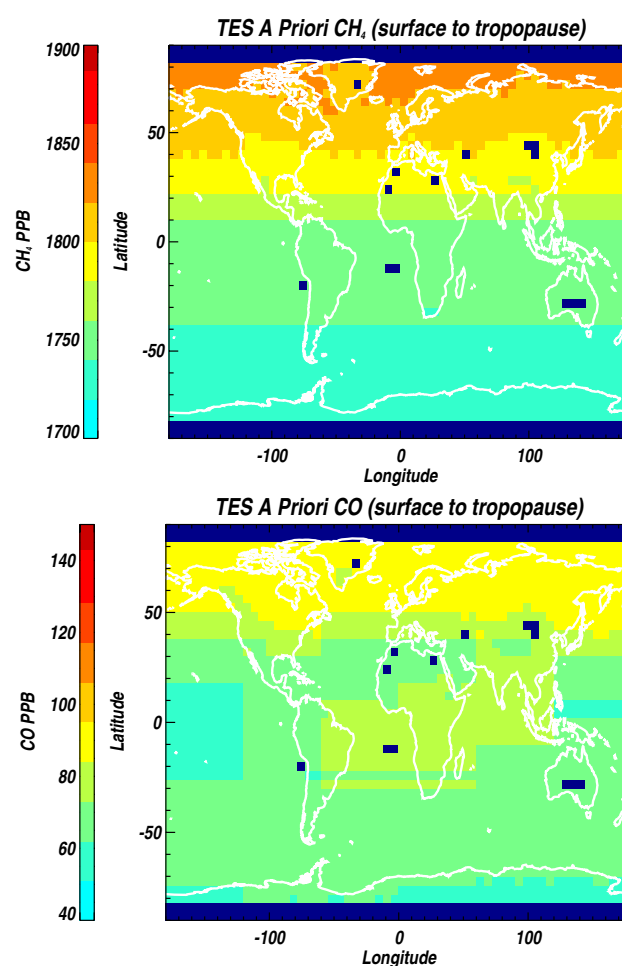


Fig. 8. (a) The TES CH₄ a priori, averaged over all pressure levels in the TES forward model in the troposphere. (b) Same as in (a) but for CO.

ations that are well above the uncertainty in the mean for a 15-degree latitudinal average. As can be seen in Figs. 1, 6, and 7, the primary differences between the TES and GEOS-Chem CH₄ estimates are typically in biomass burning outflow regions in the Southern Hemisphere or over wetlands regions in the tropical continents. However, GEOS-Chem appears to capture the methane variability over Asia and over the Indonesian peat fires as shown by the small differences between TES and GEOS-Chem over these regions. Larger mean differences (~ 10 ppb on average) between TES and GEOS-Chem are observed near the boreal forest wetland regions at high latitudes.

5 CH₄ and CO distributions in tropical fire plumes

We next examine the role of fire emissions versus emissions from other sources (e.g., wetlands and/or livestock) in the observed methane concentrations affected by the smoke plumes

from the Indonesian, South American, and African fires. For these comparisons we use the same quality flags, instrument operator, averaging, and bias correction as discussed in Sects. 4.1 and 4.2; however, because the TES tropical observations are more sensitive to CH₄ and CO variations due to increased thermal contrast in the tropics we now only use those observations that have at least 1.4 DOFS. In general, we empirically find that a profile will be uniformly sensitive to the CH₄ distribution from the lower troposphere through the tropopause for DOFS of 1.4 and above.

5.1 Indonesia

The observed distributions of CH₄ and CO for the air parcels affected by the October 2006 Indonesian fire plumes are shown in Fig. 9a. All TES observations between 80° E and 130° E and from 15° S to 5° N are included. The TES CH₄ and GEOS-Chem CO data have both been bias corrected as described in Sect. 4.3. The least-squares-derived slope for the TES data (using the data shown in Figs. 6 and 7) is 0.13 (ppb ppb⁻¹) ± 0.01 with a linear correlation coefficient (*R*) of 0.42. The uncertainty on this least-squares-derived slope is dependent on the uncertainties of the TES tropospheric CH₄ and CO tropospheric estimates that are on average 11.7 ppb and 3.7 ppb, respectively, for the observations shown here. The root-mean-square of the difference between the TES methane and CO distribution and the solid line in Fig. 9 is 13.6 ppb, indicating that a linear relationship well describes this distribution within the uncertainties of the TES data. The CH₄/CO distributions for the TES a priori are uncorrelated, as depicted in Fig. 8a, indicating that the observed correlations are from the measurement and not the a priori. The corresponding CH₄/CO distributions from the GEOS-Chem model are shown as red diamonds in Fig. 9. The slope of the GEOS-Chem CH₄/CO distribution of 0.153 ppb ppb⁻¹ ± 0.005 is higher than for the TES data but consistent (within 3 sigma) with the TES data (the error in the slope for the model distributions is calculated using the RMS spread of methane versus CO).

Part of the distribution of methane and CO observed by TES originates directly from Indonesia, while the rest is transported from elsewhere. We can gain insight into the component from Indonesian emissions by (1) comparing the TES CH₄/CO and the GEOS-Chem CH₄/CO distributions (adjusted by TES instrument operator) with the GEOS-Chem CH₄/CO distributions not adjusted by the TES instrument operator and (2) the emission ratio expected from the Indonesian emissions used as input to the GEOS-Chem model.

The slope of the GEOS-Chem CH₄/CO distribution without the TES instrument operator applied is 0.11 ppb ppb⁻¹ ± 0.005, as compared to 0.153 ± 0.005 with the TES instrument operator. Because the TES CH₄ and CO averaging kernels weight the free-tropospheric component of the GEOS-Chem distribution relative to the distribution without the TES instrument operator, this difference indicates that transport of

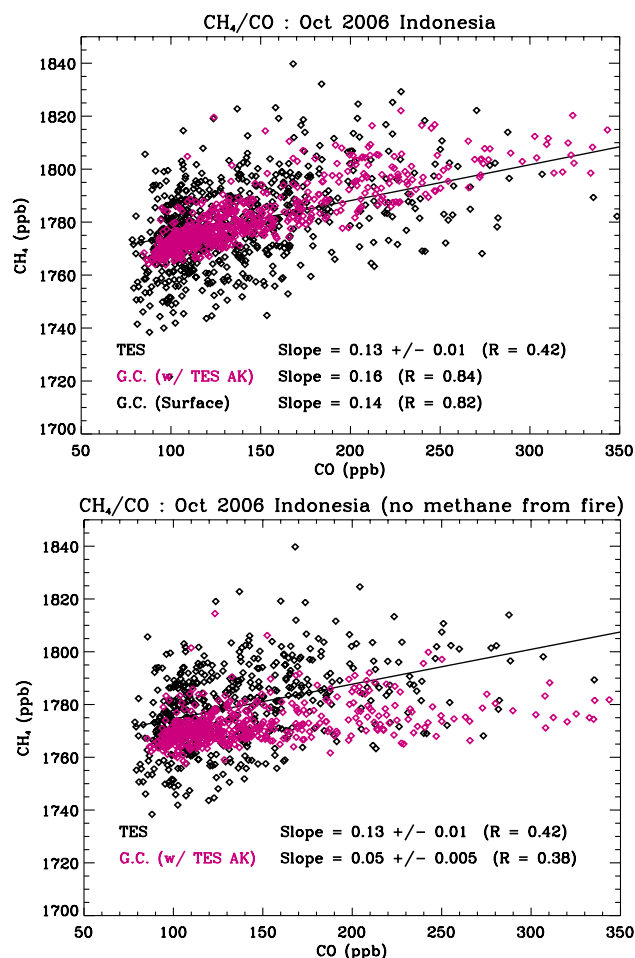


Fig. 9. (a) Distribution of CH₄ and CO over Indonesian fires. The TES data are shown in black. The GEOS-Chem data (adjusted with the TES operator) are in red. A linear fit to the TES data is shown as a black line. (b) Same as (a) but Indonesian CH₄ biomass burning emissions have been set to zero for October 2006.

methane and CO into the smoke plume contributes to the observed distribution, or else the two GEOS-Chem (with and without the TES operator) distributions would agree. We can compare this model slope of 0.11 to the value expected from the Indonesian emissions used as input to the GEOS-Chem model. Tables 1 and 2 list the CH₄ and CO emissions used in the model for Indonesia (first column) for October 2006. We only show the October 2006 period for brevity; however, the other emission sources (such as wetlands) remain approximately constant during the fall time period which includes the period of the Indonesian fire. We therefore expect from the biomass burning emissions in Tables 1 and 2 that the emission ratio of CH₄ relative to CO for the fire during October 2006 should be 2.8/43.7 or 0.064 Tg Tg⁻¹ (Andreae and Merlet, 2001), or, after accounting for a molar weight ratio of 1.75, 0.11 molecules of CH₄ per CO molecule (equivalent to ppb ppb⁻¹). This agreement between the emission ratio

Table 1. CH₄ emissions used for 2006 GEOS-Chem model estimates for October 2006.

Emission type	CH ₄ Emissions (Tg month ⁻¹)		
	Indonesia 15° S–5° N	South America 10–30° S	Southern Africa 10–30° S
Total	4.063	3.229	0.938
Gas & oil	0.203	0.082	0.018
Coal	0.031	0.004	0.096
Livestock	0.042	1.08	0.17
Waste	0.188	0.198	0.079
Biofuel	0.031	0.06	0.028
Rice	0.089	0.019	0.009
Other anthro	0.004	0.005	0.002
Biomass	2.768	0.039	0.183
Wetlands	0.688	1.641	0.27
Soil abs.	0.001	0.03	0.054
Other natural	0.019	0.101	0.084

and the modeled slope (without the TES operator) indicates that the Indonesian fire emissions largely control the GEOS-Chem CH₄/CO distributions. Recent literature suggests that peat fires should have an emission ratio of 0.099 g g⁻¹ (e.g. Christian et al., 2003; van der Werf et al., 2010), or 0.173 molecules of CH₄ per CO. These values, calculated specifically for peat fires burnt in a laboratory setting, are well outside the observed and modeled slope and indicate that the observed fire emissions are not just from peat fires but likely originate from a combination of fuel types.

We can further test how transport of nearby emissions could affect our conclusions by conducting a sensitivity study in which the CH₄ emissions from biomass burning in GEOS-Chem (Table 1) are “turned off”, or set to zero, over Indonesia during the September through November 2006 time frame, while keeping CO emissions the same (Fig. 9b). The modeled distribution is inconsistent with the observations. The modeled slope for this sensitivity study for the CH₄/CO distribution is 0.044 (ppb ppb⁻¹) ± 0.005 with a correlation of approximately 0.42. The lower value for the slope occurs because there is less emission of methane from other sources for the same amount of CO and also indicates that the enhanced methane observed over Indonesia primarily originates from the fire and not from other sources. However, the modeled CH₄/CO distribution for the case in which there are no biomass burning emissions of methane is still correlated because co-located or nearby biotic emissions in the model are transported into the smoke plume; this result is consistent with aircraft measurements of upper-tropospheric biomass burning plumes originating from Asia (e.g., Schuck et al., 2012). This correlation due to transport occurs even at the largely different observation (5 km × 8 km) and model (~ 250 km × 200 km) spatial scales because the free-tropospheric air parcels are sensitive to emissions over much larger spatial scales than the TES spatial resolution (Keppel-Aleks et al., 2011, 2012). Consequently,

Table 2. CO emissions used for GEOS-Chem model estimates for October 2006.

Emission type	CO Emissions (Tg month ⁻¹)		
	Indonesia 15° S–5° N	South America 10–30° S	Southern Africa 10–30° S
Total	45.191	2.658	5.954
Fossil fuel	1.285	0.533	0.322
Biomass	43.735	0.856	5.087
Biofuel	0	0.827	0.391
Monoterpene	0.172	0.443	0.153
Oxidation			

we conclude that part of the observed correlation is due to transport of nearby emissions into the plume.

In addition to the agreement with the slopes of the TES and GEOS-Chem CH₄/CO distributions, the RMS of the differences between the TES CH₄ observations and the VMRs of methane from the GEOS-Chem model (Fig. 7c) is 14.8 ppb, which is slightly larger than the mean TES observation error of 12.0 ppb. We therefore conclude that the emissions used for GEOS-Chem for this time period explain, within the uncertainties, the observed distribution of methane.

5.2 South America

The distribution of CH₄ and CO for air parcels affected by the South American fire plumes is shown in Fig. 10. Only data over land between –30° S and –10° S and from –70° E through –40° E are used. The slope of CH₄ versus CO is 0.47 (ppb ppb⁻¹) ± 0.04 for the TES data. The slope is 0.47 (ppb ppb⁻¹) ± 0.02 for the GEOS-Chem model estimates. The larger slopes, as compared to the slope of the CH₄/CO distribution from Indonesia, indicate that wetland emissions (or other non-fire emissions as shown in Table 1) are the primary contributors to the methane distribution for the observed air parcels (e.g., Schuck et al., 2012). This conclusion is supported by the observed CH₄ values larger than 1800 ppb for the lower CO values of approximately 90 ppb which are not expected from the GEOS-Chem model and are well above the distribution of CH₄ values in the linear fit to the TES CH₄/CO distribution. In addition, Table 1 (middle column) indicates that biomass burning emissions of methane are much smaller than other emissions.

We again performed a sensitivity test in which the methane emissions from biomass burning were set to zero for the September through November time period in GEOS-Chem. The modeled slope for the CH₄/CO distributions was reduced from 0.47 to 0.44 and the correlation was reduced to 0.81. This 0.03 difference can be compared to the emission ratio of approximately 0.05 (g g⁻¹) or 0.088 molecules of CH₄ per molecule of CO for the fire emissions used in this GEOS-Chem model. The mismatch in the reduction of the slope is due to scatter in the modeled CH₄ and CO

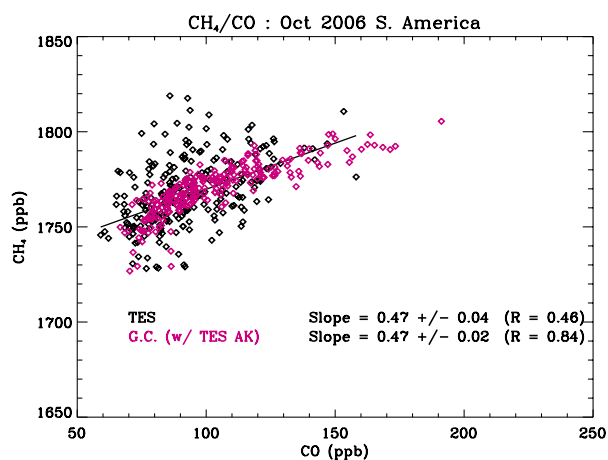


Fig. 10. Distribution of CH₄ and CO over South American fires. The TES data are shown in black. The GEOS-Chem data (adjusted with the TES operator) are in red. A linear fit to the TES data is shown as a black line.

distributions. From this analysis, we conclude that the correlation between CO and CH₄ is primarily driven by transport of nearby wetland emissions or other sources (e.g., livestock) into the observed air parcels.

Because wetlands and livestock (or other non-fire emissions) are the primary contributors to the distribution of CH₄ over this region (middle column Table 1) it is more difficult to place direct constraints on the total methane emissions and those due to biomass burning for this region and for this time period. However, this analysis suggests that CO might be a useful transport tracer for placing constraints on total methane emissions as demonstrated for CO₂ fluxes (e.g., Palmer et al., 2006; Wang et al., 2009). Alternatively, observations in the change of the slope of the CH₄/CO distribution over “short” time periods might provide constraints on biomass burning over this region if we assume that non-fire emissions remain approximately constant over the “short” time period. We will test these approaches in subsequent research.

5.3 Southern Africa

In general, African biomass burning contributes the most to the distribution of tropospheric CO relative to other tropical regions (e.g., Edwards et al., 2006). However, during the fall 2006 time period emissions from this region are less than from Indonesia as expected from the GEOS-Chem model inputs in Table 2 and the TES CO observations. The distribution of CH₄ and CO for the air parcels affected by the African fire plumes are shown in Fig. 11. Only data between -30° S and -10° S and from 10° E through 45° E are used. The slope for the TES CH₄/CO distribution is 0.44 (ppb ppb⁻¹) ± 0.03 with a correlation of $R = 0.42$. The slope for the CH₄/CO distribution from GEOS-Chem is 0.46 (ppb ppb⁻¹) ± 0.03 for the average tropospheric model estimates. The fact that the

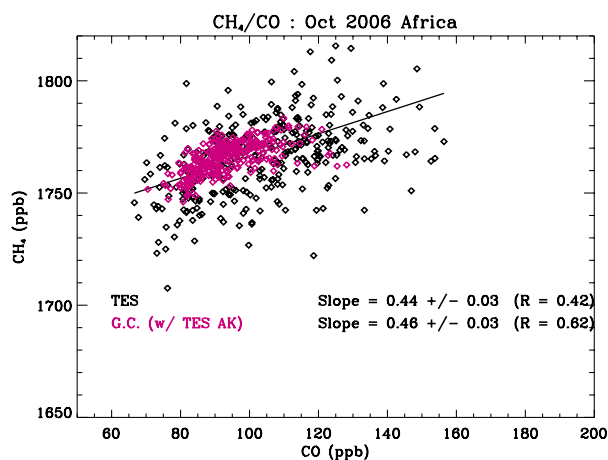


Fig. 11. Distribution of CH₄ and CO over African fires. The TES data are shown in black. The GEOS-Chem data (adjusted with the TES operator) are in red. A linear fit to the TES data is shown as a black line.

differences between TES and GEOS-Chem are larger than the mean observation error in each grid box also indicates that the sources of these methane and CO enhancements are not well quantified. Subsequent analysis and data will be needed to place constraints on the methane budget in this region.

6 Summary

In this paper we use new free-tropospheric CH₄ observations from the Aura TES satellite instrument to place constraints on methane emissions from tropical fires during the 2006 El Niño when there were strong peat fires over Indonesia as well as fires over South America and southern Africa. We first evaluated the global distribution of free-tropospheric CH₄ and CO from Aura TES observations against the GEOS-Chem model for October 2006 to ensure that the model could be used to interpret the data. We find that the TES CH₄ is biased high relative to the GEOS-Chem CH₄ distributions by approximately 26.3 ppb, consistent with previous validation studies involving the HIPPO aircraft campaign (Wecht et al., 2012). This bias is nearly uniform for latitudes between 50° S and 80° N; higher biases south of 50° S are likely a result of inconsistencies in the tropopause height between the TES and GEOS-Chem stratospheric CH₄ distributions.

We find that the slopes of the TES and GEOS-Chem CH₄/CO distributions for the Indonesian peat fires and over South America and southern Africa (30° S to 10° S) are consistent (within the error of the slope). In addition, the TES methane observations and the GEOS-Chem methane distributions are consistent (within the TES data uncertainty) for air parcels affected by the Indonesian peat fire plumes. We therefore conclude that the relative distribution of emissions from fires versus biotic emissions in GEOS-Chem explains

the relative distribution of the TES CH₄ and CO observations. Over Indonesia, an observed slope of 0.13 (ppb ppb⁻¹) ± 0.01, as compared to a modeled slope of 0.15 (ppb ppb⁻¹) ± 0.005 and an emission ratio of 0.11, indicates that most of the observed methane in the fire plumes over Indonesia came from the fires. A sensitivity study in which biomass burning emissions of methane are turned off in GEOS-Chem supports this conclusion because the modeled (no methane from biomass burning) CH₄/CO distribution becomes 0.045 (ppb ppb⁻¹) ± 0.005. However this sensitivity study also indicates that a component of this distribution is due to transport of non-fire emissions into the observed plume. Finally, laboratory measurements of peat fire plumes (Christian et al., 2003) have an emission ratio of approximately 0.18, which is much larger than the emission ratio used in this study, indicating that the Indonesian fires plumes have a combination of peat and non-peat sources. Because we can attribute most of the enhanced methane in these Indonesian fire plume to the actual fire and not to other emissions, it is likely that we can place direct constraints on the methane emissions from the fire by using estimates of CO emissions such as might be obtained from the near-surface CO estimates from the Terra MOPITT satellite (e.g., Worden et al., 2010); this will be the subject of a subsequent study.

Unlike the Indonesian CH₄/CO distributions, the slopes of the air parcels affected by fire plumes over South American and southern African regions are much larger (slopes ~ 0.47 ± 0.04 and 0.44 ± 0.03, respectively, units of ppb ppb⁻¹) than the slope expected from biomass burning alone even though the CH₄ and CO distributions are correlated ($R \sim 0.46$ and 0.42 , respectively). By conducting a sensitivity study in which biomass burning sources of methane were “turned off” in the GEOS-Chem model during the observation time frame, we conclude that transport of nearby biotic (e.g., wetland and livestock) emissions into the observed air parcels is the primary contributor to atmospheric CH₄ in these observed air parcels. Further investigation is therefore needed to better constrain fire-based methane emissions over these regions during this time period. For example, changes in the observed CH₄/CO slope during peak fire season might be useful for placing constraints on methane emissions from these fires. We will also test whether CO can be used as a transport tracer to constrain CH₄ emissions as studied for CO₂ fluxes by Palmer et al. (2006) and Wang et al. (2009).

Acknowledgements. Part of this research was carried out at the Jet Propulsion Laboratory, California Institute of Technology, under a contract with the National Aeronautics and Space Administration. The authors would like to thank Peter Bergamaschi for providing TM5 CH₄ distributions which helped to initiate this analysis. Daniel Jacob (Harvard University) kindly provided a review of this manuscript prior to submission.

Edited by: R. McLaren

References

- Andreae, M. O. and Merlet, P.: Emission of trace gases and aerosols from biomass burning, *Global Biogeochem. Cycles*, 15, 955–966, 2001.
- Beer, R., Glavich, T. A. and Rider, D. M.: Tropospheric emission spectrometer for the Earth Observing System’s Aura satellite, *Appl. Optics*, 40, 2356–2367, 2001.
- Bey, I., Jacob, D., Yantosca, R., Logan, J., Field, B., Fiore, A., Li, Q., Liu, H. Y., Mickley, L., and Schultz, M. G.: Global modeling of tropospheric chemistry with assimilated meteorology: Model description and evaluation, *J. Geophys. Res.-Atmos.*, 106, 23073–23095, 2001.
- Bloom, A. A., Palmer, P. I., Fraser, A., Reay, D. S. and Frankenberg, C.: Large-Scale Controls of Methanogenesis Inferred from Methane and Gravity Spaceborne Data, *Science*, 327, 322–325, doi:10.1126/science.1175176, 2010.
- Bousquet, P., Ciais, P., Miller, J. B., Dlugokencky, E. J., Hauglustaine, D. A., Prigent, C., Van Der Werf, G. R., Peylin, P., Brunke, E.-G., Carouge, C., Langenfelds, R. L., Lathière, J., Papa, F., Ramonet, M., Schmidt, M., Steele, L. P., Tyler, S. C., and White, J.: Contribution of anthropogenic and natural sources to atmospheric methane variability, *Nature*, 443, 439–443, doi:10.1038/nature05132, 2006.
- Bousquet, P., Ringeval, B., Pison, I., Dlugokencky, E. J., Brunke, E.-G., Carouge, C., Chevallier, F., Fortems-Cheiney, A., Frankenberg, C., Hauglustaine, D. A., Krummel, P. B., Langenfelds, R. L., Ramonet, M., Schmidt, M., Steele, L. P., Szopa, S., Yver, C., Viovy, N., and Ciais, P.: Source attribution of the changes in atmospheric methane for 2006–2008, *Atmos. Chem. Phys.*, 11, 3689–3700, doi:10.5194/acp-11-3689-2011, 2011.
- Bowman, K. W., Rodgers, C. D., Kulawik, S. S., Worden, J., Sarkissian, E., Osterman, G., Steck, T., Lou, M., Eldering, A., Shephard, M., Worden, H., Lampel, M., Clough, S., Brown, P., Rinsland, C., Gunson, M., and Beer, R.: Tropospheric Emission Spectrometer: Retrieval Method and Error Analysis, *IEEE T. Geosci. Remote Sens.*, 44, 1297–1307, doi:10.1109/TGRS.2006.871234, 2006.
- Christian, T. J.: Comprehensive laboratory measurements of biomass-burning emissions: 1. Emissions from Indonesian, African, and other fuels, *J. Geophys. Res.*, 108, 4719, doi:10.1029/2003JD003704, 2003.
- Clough, S. A., Shephard, M. W., Worden, J., Brown, P. D., Worden, H. M., Luo, M., Rodgers, C. D., Rinsland, C. P., Goldman, A. and Brown, L.: Forward model and Jacobians for tropospheric emission spectrometer retrievals, *IEEE T. Geosci. Remote Sens.*, 44, 1308–1323, 2006.
- Crevoisier, C., Nobileau, D., Fiore, A. M., Armante, R., Chédin, A., and Scott, N. A.: Tropospheric methane in the tropics – first year from IASI hyperspectral infrared observations, *Atmos. Chem. Phys.*, 9, 6337–6350, doi:10.5194/acp-9-6337-2009, 2009.
- Deeter, M. N., Worden, H. M., Gille, J. C., Edwards, D. P., Mao, D., and Drummond, J. R.: MOPITT multispectral CO retrievals: Origins and effects of geophysical radiance errors, *J. Geophys. Res.*, 116, D15303, doi:10.1029/2011JD015703, 2011.
- Deeter, M. N., Worden, H. M., Edwards, D. P., Gille, J. C., and Andrews, A. E.: Evaluation of MOPITT retrievals of lower-tropospheric carbon monoxide over the United States, *J. Geophys. Res.*, 117, D13306, doi:10.1029/2012JD017553, 2012.

- Denman, K. L., Brasseur, G., Chidthaisong, A., Ciais, P., Cox, P. M., Dickinson, R. E., Hauglustaine, D., Heinze, C., Holland, E., Jacob, D., Lohmann, U., Ramachandran, S., da Silva Dias, P. L., Wofsy, S. C., and Zhang X.: Couplings Between Changes in the Climate System and Biogeochemistry, in: *Climate Change 2007: The Physical Science Basis. Contribution of Working Group I to the Fourth Assessment Report of the Intergovernmental Panel on Climate Change*, edited by: Solomon, S., Qin, D., Manning, M., Chen, Z., Marquis, M., Averyt, K. B., Tignor, M., and Miller, H. L., Cambridge University Press, Cambridge, United Kingdom and New York, NY, USA, 2007.
- Dlugokencky, E. J., Bruhwiler, L., White, J. W. C., Emmons, L. K., Novelli, P. C., Montzka, S. A., Masarie, K. A., Lang, P. M., Crotwell, A. M., Miller, J. B., and Gatti, L. V.: Observational constraints on recent increases in the atmospheric CH₄ burden, *Geophys. Res. Lett.*, 36, L18803, doi:10.1029/2009GL039780, 2009.
- Dlugokencky, E. J., Nisbet, E. G., Fisher, R., and Lowry, D.: Global atmospheric methane: budget, changes and dangers, *Philos. T. Roy. Soc. A*, 369, 2058–2072, doi:10.1098/rsta.2010.0341, 2011.
- Edwards, D. P., Pétron, G., Novelli, P. C., Emmons, L. K., Gille, J. C., and Drummond, J. R.: Southern Hemisphere carbon monoxide interannual variability observed by Terra/Measurement of Pollution in the Troposphere (MOPITT), *J. Geophys. Res.*, 111, D16303, doi:10.1029/2006JD007079, 2006.
- Eldering, A., Kulawik, S. S., Worden, J., Bowman, K., and Osterman, G.: Implementation of cloud retrievals for TES atmospheric retrievals: 2. Characterization of cloud top pressure and effective optical depth retrievals, *J. Geophys. Res.*, 113, D16S37, doi:10.1029/2007JD008858, 2008.
- European Commission, Joint Research Centre (JRC)/Netherlands Environmental Assessment Agency (PBL). Emission Database for Global Atmospheric Research (EDGAR), release version 4.0, <http://edgar.jrc.ec.europa.eu>, 2009
- Forster, P., Ramaswamy, V., Artaxo, P., Berntsen, T., Betts, R., Fahey, D. W., Haywood, J., Lean, J., Lowe, D. C., Myhre, G., Nganga, J., Prinn, R., Raga, G., Schulz, M., and Van Dorland, R.: Changes in Atmospheric Constituents and in Radiative Forcing, in: *Climate Change 2007: The Physical Science Basis. Contribution of Working Group I to the Fourth Assessment Report of the Intergovernmental Panel on Climate Change*, edited by: Solomon, S., Qin, D., Manning, M., Chen, Z., Marquis, M., Averyt, K. B., Tignor, M., and Miller, H. L., Cambridge University Press, Cambridge, United Kingdom and New York, NY, USA, 2007
- Frankenberg, C., Meirink, J., Van Weele, M., Platt, U., and Wagner, T.: Assessing methane emissions from global space-borne observations, *Science*, 308, 1010–1014, doi:10.1126/science.1106644, 2005.
- Frankenberg, C., Aben, I., Bergamaschi, P., Dlugokencky, E. J., van Hees, R., Houweling, S., van der Meer, P., Snel, R., and Tol, P.: Global column-averaged methane mixing ratios from 2003 to 2009 as derived from SCIAMACHY: Trends and variability, *J. Geophys. Res.*, 116, D04302, doi:10.1029/2010JD014849, 2011.
- Fung, I., Prather, M., John, J., Lerner, J., and Matthews, E.: Three-dimensional model synthesis of the global methane cycle, *J. Geophys. Res.*, 96, 13033–13065, 1991.
- Gonzi, S. and Palmer, P. I.: Vertical transport of surface fire emissions observed from space, *J. Geophys. Res.*, 115, D02306, doi:10.1029/2009JD012053, 2010.
- Ho, S.-P., Edwards, D. P., Gille, J. C., Luo, M., Osterman, G. B., Kulawik, S. S., and Worden, H.: A global comparison of carbon monoxide profiles and column amounts from Tropospheric Emission Spectrometer (TES) and Measurements of Pollution in the Troposphere (MOPITT), *J. Geophys. Res.*, 114, D21307, doi:10.1029/2009JD012242, 2009.
- Kaplan, J. O.: Wetlands at the Last Glacial Maximum: Distribution and methane emissions, *Geophys. Res. Lett.*, 29, 1079, doi:10.1029/2001GL013366, 2002.
- Keppel-Aleks, G., Wennberg, P. O., and Schneider, T.: Sources of variations in total column carbon dioxide, *Atmos. Chem. Phys.*, 11, 3581–3593, doi:10.5194/acp-11-3581-2011, 2011.
- Keppel-Aleks, G., Wennberg, P. O., Washenfelder, R. A., Wunch, D., Schneider, T., Toon, G. C., Andres, R. J., Blavier, J.-F., Connor, B., Davis, K. J., Desai, A. R., Messerschmidt, J., Notholt, J., Roehl, C. M., Sherlock, V., Stephens, B. B., Vay, S. A., and Wofsy, S. C.: The imprint of surface fluxes and transport on variations in total column carbon dioxide, *Biogeosciences*, 9, 875–891, doi:10.5194/bg-9-875-2012, 2012.
- Kirchstetter, T. W., Novakov, T., and Hobbs, P. V.: Evidence that the spectral dependence of light absorption by aerosols is affected by organic carbon, *J. Geophys. Res.*, 109, D21208, doi:10.1029/2004JD004999, 2004.
- Kulawik, S. S., Worden, J., Eldering, A., Bowman, K., Gunson, M., Osterman, G. B., Zhang, L., Clough, S. A., Shephard, M. W., and Beer, R.: Implementation of cloud retrievals for Tropospheric Emission Spectrometer (TES) atmospheric retrievals: part 1. Description and characterization of errors on trace gas retrievals, *J. Geophys. Res.*, 111, D24204, doi:10.1029/2005JD006733, 2006.
- Lelieveld, J., Crutzen, P. J., and Dentener, F. J.: Changing concentration, lifetime and climate forcing of atmospheric methane, *Tellus*, 50, 128–150, 1998.
- Logan, J. A., Megretskaya, I., Nassar, R., Murray, L. T., Zhang, L., Bowman, K. W., Worden, H. M., and Luo, M.: Effects of the 2006 El Niño on tropospheric composition as revealed by data from the Tropospheric Emission Spectrometer (TES), *Geophys. Res. Lett.*, 35, L03816, doi:10.1029/2007GL031698, 2008.
- Luo, M., rinsland, C., Fisher, B., Sachse, G., Diskin, G., Logan, J., Worden, H., Kulawik, S., Osterman, G., Eldering, A., Herman, R., Shephard, M.: TES carbon monoxide validation with DACOM aircraft measurements during INTEX-B 2006, *J. Geophys. Res.*, 112, D24S48, doi:10.1029/2007JD008803, 2007.
- Luo, M., Boxe, C., Jiang, J., Nassar, R., and Livesey, N.: Interpretation of Aura satellite observations of CO and aerosol index related to the December 2006 Australia fires, *Remote Sens. Environ.*, 114, 2853–2862, doi:10.1016/j.rse.2010.07.003, 2010.
- Nassar, R., Logan, J. A., Megretskaya, I. A., Murray, L. T., Zhang, L., and Jones, D. B. A.: Analysis of tropical tropospheric ozone, carbon monoxide, and water vapor during the 2006 El Niño using TES observations and the GEOS-Chem model, *J. Geophys. Res.*, 114, D17304, doi:10.1029/2009JD011760, 2009.
- O'Connor, F. M., Boucher, O., Gedney, N., Jones, C. D., Folberth, G. A., Coppel, R., Friedlingstein, P., Collins, W. J., Chappellaz, J., Ridley, J. and Johnson, C. E.: Possible role of wetlands, permafrost, and methane hydrates in the methane cycle under future climate change: A review, *Rev. Geophys.*, 48, RG4005, doi:10.1029/2010RG000326, 2010.

- Palmer, P. I., Suntharalingam, P., Jones, D. B. A., Jacob, D. J., Streets, D. G., Fu, Q., Vay, S. A., and Sachse, G. W.: Using CO₂: CO correlations to improve inverse analyses of carbon fluxes, *J. Geophys. Res.*, 111, D12318, doi:10.1029/2005JD006697, 2006.
- Page, S. E., Siegert, F., Rieley, J. O., Boehm, H. D. V., Jaya, A., and Limin, S.: The amount of carbon released from peat and forest fires in Indonesia during 1997, *Nature*, 420, 61–65, 2002.
- Park, R. J.: Natural and transboundary pollution influences on sulfate-nitrate-ammonium aerosols in the United States: Implications for policy, *J. Geophys. Res.*, 109, D15204, doi:10.1029/2003JD004473, 2004.
- Pétron, G., Frost, G., Miller, B. R., Hirsch, A. I., Montzka, S. A., Karion, A., Trainer, M., Sweeney, C., Andrews, A. E., Miller, L., Kofler, J., Bar-Ilan, A., Dlugokencky, E. J., Patrick, L., Moore, C. T., Jr., Ryerson, T. B., Siso, C., Kolodzey, W., Lang, P. M., Conway, T., Novelli, P., Masarie, K., Hall, B., Guenther, D., Kitzis, D., Miller, J., Welsh, D., Wolfe, D., Neff, W., and Tans, P.: Hydrocarbon emissions characterization in the Colorado Front Range: A pilot study, *J. Geophys. Res.*, 117, D04304, doi:10.1029/2011JD016360, 2012.
- Pickett-Heaps, C. A., Jacob, D. J., Wecht, K. J., Kort, E. A., Wofsy, S. C., Diskin, G. S., Worthy, D. E. J., Kaplan, J. O., Bey, I., and Drevet, J.: Magnitude and seasonality of wetland methane emissions from the Hudson Bay Lowlands (Canada), *Atmos. Chem. Phys.*, 11, 3773–3779, doi:10.5194/acp-11-3773-2011, 2011.
- Prinn, R. G., Huang, J., Weiss, R. F., Cunnold, D. M., Fraser, P. J., Simmonds, P. G., McCulloch, A., Harth, C., Reimann, S., and Salameh, P.: Evidence for variability of atmospheric hydroxyl radicals over the past quarter century, *Geophys. Res. Lett.*, 32, L07809, doi:10.1029/2004GL022228, 2005.
- Rigby, M., Prinn, R. G., Fraser, P. J., Simmonds, P. G., Langenfelds, R. L., Huang, J., Cunnold, D. M., Steele, L. P., Krummel, P. B., Weiss, R. F., O'doherty, S., Salameh, P. K., Wang, H. J., Harth, C. M., Mühle, J., and Porter, L. W.: Renewed growth of atmospheric methane, *Geophys. Res. Lett.*, 35, L22805, doi:10.1029/2008GL036037, 2008.
- Rodgers, C. D.: *Inverse Methods for Atmospheric Sounding: Theory and Practice*, World Scientific Publishing Co., Singapore, 2000.
- Rodgers, C. D. and Connor, B. J.: Intercomparison of remote sounding instruments, *J. Geophys. Res.-Atmos.*, 108, 4116, doi:10.1029/2002JD002299, 2003.
- Schuck, T. J., Ishijima, K., Patra, P. K., Baker, A. K., Machida, T., Matsueda, H., Sawa, Y., Umezawa, T., Brenninkmeijer, C. A. M., and Lelieveld, J.: Distribution of methane in the tropical upper troposphere measured by CARIBIC and CONTRAIL aircraft, *J. Geophys. Res.*, 117, D19304, doi:10.1029/2012JD018199, 2012.
- Shindell, D., Kuylenstierna, J. C. I., Vignati, E., Van Dingenen, R., Amann, M., Klimont, Z., Anenberg, S. C., Muller, N., Janssens-Maenhout, G., Raes, F., Schwartz, J., Faluvegi, G., Pozzoli, L., Kupiainen, K., Hoglund-Isaksson, L., Emberson, L., Streets, D., Ramanathan, V., Hicks, K., Oanh, N. T. K., Milly, G., Williams, M., Demkine, V., and Fowler, D.: Simultaneously Mitigating Near-Term Climate Change and Improving Human Health and Food Security, *Science*, 335, 183–189, doi:10.1126/science.1210026, 2012.
- van der Werf, G. R., Randerson, J. T., Giglio, L., Collatz, G. J., Kasibhatla, P. S., and Arellano Jr., A. F.: Interannual variability in global biomass burning emissions from 1997 to 2004, *Atmos. Chem. Phys.*, 6, 3423–3441, doi:10.5194/acp-6-3423-2006, 2006.
- van der Werf, G. R., Randerson, J. T., Giglio, L., Collatz, G. J., Mu, M., Kasibhatla, P. S., Morton, D. C., DeFries, R. S., Jin, Y., and van Leeuwen, T. T.: Global fire emissions and the contribution of deforestation, savanna, forest, agricultural, and peat fires (1997–2009), *Atmos. Chem. Phys.*, 10, 11707–11735, doi:10.5194/acp-10-11707-2010, 2010.
- Verma, S., Worden, J., Pierce, B., Jones, D. B. A., Al-Saadi, J., Boersma, F., Bowman, K., Eldering, A., Fisher, B., Jourdain, L., Kulawik, S., Worden, H.: Ozone production in boreal fire smoke plumes using observations from the Tropospheric Emission Spectrometer and the Ozone Monitoring Instrument, *J. Geophys. Res.*, 114, D02303, doi:10.1029/2008JD010108, 2009.
- Wang, H., Jacob, D. J., Kopacz, M., Jones, D. B. A., Suntharalingam, P., Fisher, J. A., Nassar, R., Pawson, S., and Nielsen, J. E.: Error correlation between CO₂ and CO as constraint for CO₂ flux inversions using satellite data, *Atmos. Chem. Phys.*, 9, 7313–7323, doi:10.5194/acp-9-7313-2009, 2009.
- Wang, J. S., Logan, J. A., McElroy, M. B., Duncan, B. N., Megretskaiia, I. A., and Yantosca, R. M.: A 3-D model analysis of the slowdown and interannual variability in the methane growth rate from 1988 to 1997, *Global Biogeochem. Cy.*, 18, GB3011, doi:10.1029/2003GB002180, 2004.
- Wecht, K. J., Jacob, D. J., Wofsy, S. C., Kort, E. A., Worden, J. R., Kulawik, S. S., Henze, D. K., Kopacz, M., and Payne, V. H.: Validation of TES methane with HIPPO aircraft observations: implications for inverse modeling of methane sources, *Atmos. Chem. Phys.*, 12, 1823–1832, doi:10.5194/acp-12-1823-2012, 2012.
- Worden, J., Kulawik, S., Shepard, M., Clough, S., Worden, H., Bowman, K., and Goldman, A.: Predicted errors of tropospheric emission spectrometer nadir retrievals from spectral window selection, *J. Geophys. Res.*, 109, D09308, doi:10.1029/2004JD004522, 2004.
- Worden, H. M., Deeter, M. N., Edwards, D. P., Gille, J. C., Drummond, J. R., and Nedelec, P.: Observations of near-surface carbon monoxide from space using MOPITT multispectral retrievals, *J. Geophys. Res.*, 115, D18314, doi:10.1029/2010JD014242, 2010.
- Worden, J., Kulawik, S., Frankenberg, C., Payne, V., Bowman, K., Cady-Peirara, K., Wecht, K., Lee, J.-E., and Noone, D.: Profiles of CH₄, HDO, H₂O, and N₂O with improved lower tropospheric vertical resolution from Aura TES radiances, *Atmos. Meas. Tech.*, 5, 397–411, doi:10.5194/amt-5-397-2012, 2012.
- Xiong, X., Houweling, S., Wei, J., Maddy, E., Sun, F., and Barnett, C.: Methane plume over south Asia during the monsoon season: satellite observation and model simulation, *Atmos. Chem. Phys.*, 9, 783–794, doi:10.5194/acp-9-783-2009, 2009.